MOLECULAR AND CELLULAR BIOLOGY, Aug. 2002, p. 5923–5937 Vol. 22, No. 16
0270-7306/02/$04.00+0 DOI: 10.1128/MCB.22.16.5923–5937.2002

The Function of TIF2/GRIP1 in Mouse Reproduction Is Distinct from Those of SRC-1 and p/CIP

Martine Gehin, Manuel Mark, Christine Dennefeld, Andrée Dierich, Hinrich Gronemeyer, and Pierre Chambon*

Institut de Génétique et de Biologie Moléculaire et Cellulaire (IGBMC), CNRS/INSERM/ULP/Collège de France, 67404 Illkirch Cedex, France

Received 18 March 2002/Accepted 30 April 2002

Human TIF2 (hTIF2) is a member of the p160 family of nuclear receptor coactivators, which includes SRC-1 and p/CIP. Although the functions of hTIF2 and of its mouse homolog (GRIP1 or mTIF2) have been clearly established in vitro, their physiological role remains elusive. Here, we have generated mice lacking mTIF2/GRIP1 and examined their phenotype with a particular emphasis on reproductive functions. TIF2$^{-/-}$ mice are viable, but the fertility of both sexes is impaired. Male hypofertility is due to defects in both spermiogenesis (teratozoospermia) and age-dependent testicular degeneration, and TIF2 expression appears to be essential for adhesion of Sertoli cells to germ cells. Female hypofertility is due to a placental hypoplasia that most probably reflects a requirement for maternal TIF2 in decidua stromal cells that face the developing placenta. We conclude that TIF2 plays a critical role in mouse reproductive functions, whereas previous reports have not revealed serious fertility impairment in SRC-1$^{-/-}$ or p/CIP$^{-/-}$ mutants. Thus, even though the three p160 coactivators exhibit strong sequence homology and similar activity in assays in vitro, they play distinct physiological roles in vivo, as their genetic eliminations result in distinct pathologies.

Transcription factors play a major role in the remodeling of the chromatin nucleosomal structure in regions that include gene promoters, and histone acetyl transferases (HATs) are essential in this remodeling (33, 70). Several general coactivators, e.g., cAMP response element binding (CREB) protein (CBP)/p300 and p300/CBP-associated protein factor (PCAF), recruited in the presence of agonistic ligands by nuclear receptors (NRs) to mediate their transcriptional activation functions, have intrinsic HAT activity (5, 9). These general coactivators can also be recruited by interaction with more specific coactivators, such as members of the p160 coactivator family (steroid receptor coactivator 1 [SRC-1] [49], transcriptional intermediary factor 2 [TIF2]/GRIP1/SRC-2 [27, 64] and CBP-interacting protein [pCIP]/ACTR/AIB1/RAC3/TRAM1/SRC-3 [3, 17, 38, 61, 62]), which efficiently bind to NRs in an agonistic ligand-dependent manner, and may also exhibit HAT activity on their own (22, 44, 69, 74). In contrast and in a context-dependent manner, TIF2 has also been recently shown to potentiate repression mediated by the glucocorticoid hormone receptor in the presence of a glucocorticoid receptor agonist, but not antagonist (54).

The three members of the p160 coactivator family share 40% overall sequence identity. In vitro and cultured cell transfection studies have shown that a centrally located NR interaction domain (NID) is present in all three members of the family. The NID contains three LXXLL motifs (the NR binding boxes) that specifically interact with the AF-2 activation domain of NRs through a hydrophobic site located on the surface of agonist-activated ligand binding domains (11). It has also been shown that two autonomous transcriptional activation domains (AD1 and AD2) are found in each of the p160 proteins. AD1 encompasses the binding site of the general coactivators CBP/p300 (65), while AD2 interacts with the protein methylase coactivator-associated arginine methyltransferase 1 (CARM1) and other factors (16, 29, 32; for reviews, see references 22, 37, 44, 53, and 74).

Cell transfection studies and some compensatory overexpression of mTIF2 (the mouse homolog of human TIF2, also known as GRIP1) in certain SRC-1 KO mutant tissues have suggested the existence of a partial functional redundancy between members of the p160 family (73). However, there is genetic evidence that the three members of the p160 family are differentially involved in the physiological functions of NR signaling in vivo. Analysis of SRC1-null mice has shown that, while both male and female SRC1 knockout (KO) mice are viable and fertile, they exhibit partial resistance to several hormones, including estrogen, progestin, androgen, and thyroid hormones (67, 73). Elimination of p/CIP has revealed that it is required for normal mouse growth (66, 72), as well as for some female reproductive functions (72), and the human homolog of p/CIP (AIB1) has been found to be strongly amplified and/or overexpressed in 64% of primary breast cancer and some primary ovarian tumors (7). Furthermore, translocation between the TIF2 gene and the MOZ gene encoding a HAT protein (15) has been identified in human acute myeloid leukemia (14).

We report here some of the physiological functions of the mouse TIF2 coactivator, which are revealed by the analysis of TIF2-null animals. Our results show that TIF2 plays a critical role in the reproductive functions of the mouse as, in contrast to SRC-1 and p/CIP KO mice, the fertility of both male and female TIF2 KO mice is impaired. Thus, even though the p160

* Corresponding author. Mailing address: Institut de Génétique et de Biologie Moléculaire et Cellulaire (IGBMC), CNRS/INSERM/ULP/Collège de France, B.P. 163, 67404 Illkirch Cedex, France. Phone: 33 3 88 65 32 13. Fax: 33 3 88 65 32 03. E-mail: chambon@igbmc.u-strasbg.fr.

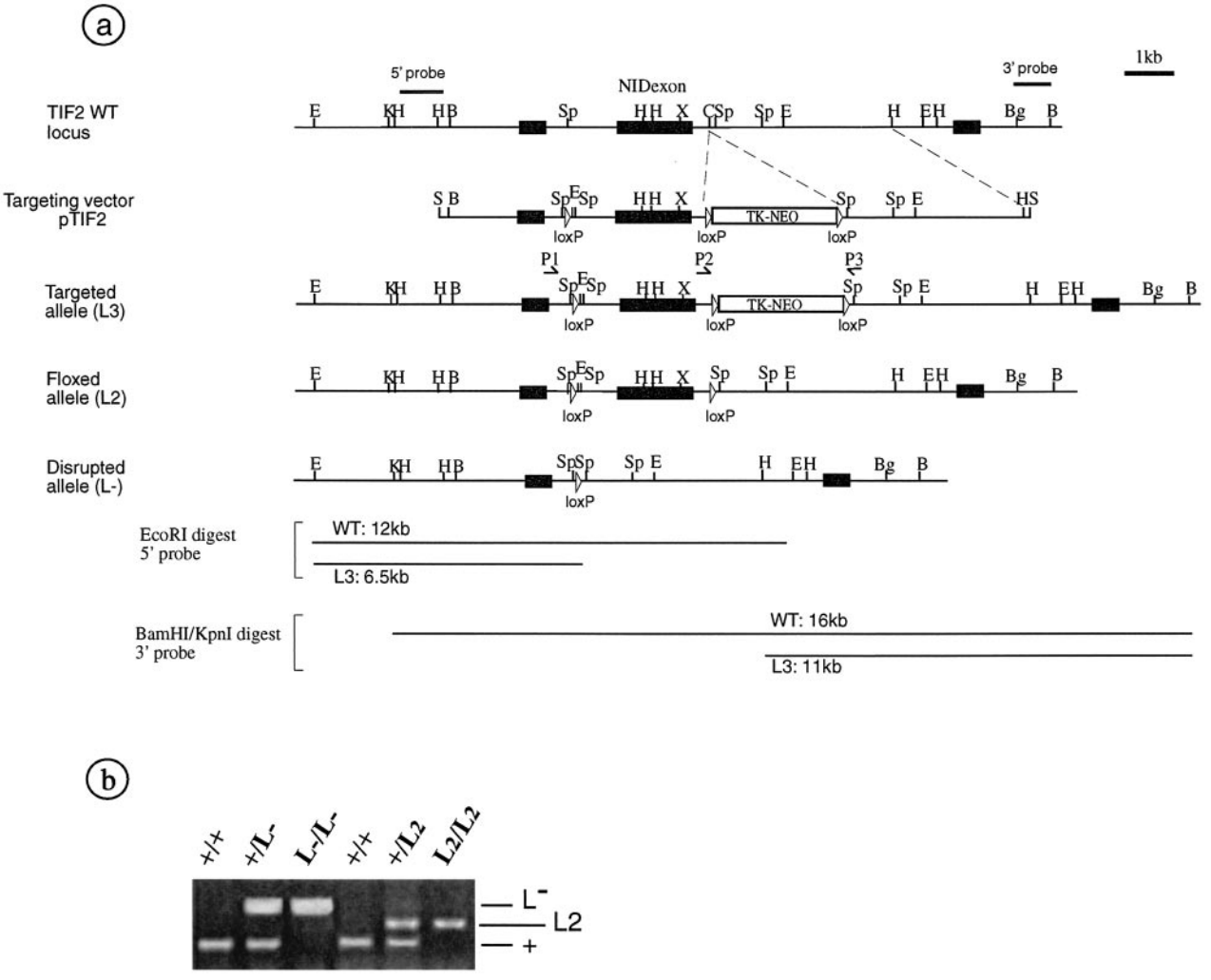

FIG. 1. Targeted disruption of the mouse TIF2 gene. (A) Schematic strategy to generate TIF2 KO mice: diagrams showing the WT TIF2 locus, the targeting vector, the targeted allele L3, the floxed allele L2, and the allele with L^- deleted after Cre-mediated recombination. The exon containing the NID is shown as the NIDexon black box. The location of 5′ and 3′ probes is indicated. The TK-neo cassette is shown and loxP sites are indicated with open triangles. Arrows indicate the positions of PCR primers (P1, P2, and P3) used for DNA genotyping. The size of restriction fragments obtained by Southern blot is given in kilobases. Abbreviations: E, *Eco*RI; K, *Kpn*I; H, *Hin*dIII; B, *Bam*HI; Sp, *Spe*I; X, *Xho*I; C, *Cla*I; Bg, *Bgl*II; S, *Sac*I. (B) PCR diagnosis (see Materials and Methods) used to genotype the mice.

coactivators exhibit significant structural homologies and may be partially functionally redundant, they exert different physiological functions, as their absence results in distinct pathologies.

MATERIALS AND METHODS

Generation of TIF2 mutant mice. Mouse TIF2 genomic clones were obtained by screening a 129/Sv embryonic stem (ES) cell DNA library, with a mouse TIF2 (GRIP1) cDNA probe. A targeting vector was generated from two overlapping genomic fragments containing the exon encoding the three NR boxes of the NID (nucleotides 1330 to 2597 [accession number U39060]) (Fig. 1a). The TK-neo cassette from pHR56 (46) was cloned into the *Cla*I site, and a LoxP site followed by an *Eco*RI site was introduced at the *Spe*I site by PCR-based site-directed mutagenesis (Fig. 1a). The *Bam*HI-*Hin*dIII fragment of the targeting vector (Fig. 1a) was electroporated into 129/SvPas H1 ES cells (20), and G418 neomycin-resistant clones were expanded (40).

ES cells containing a targeted TIF2 L3 allele were identified by Southern blot analysis of (i) *Bam*HI-digested ES cell genomic DNA using a 5′ (P5′) external probe and (ii) *Bam*HI- and *Kpn*I-digested ES cell genomic DNA using a 3′ (P3′) external probe and a neomycin probe (Fig. 1a). Targeted ES cells were injected into C57BL/6 blastocysts which were implanted in a pseudopregnant host of the same strain. Chimeric males were obtained that transmitted the mutation through crosses with C57BL/6 females, yielding heterozygous $TIF2^{L3/+}$ mice (mice with an L3 allele and a wild-type [WT] allele). $TIF2^{L3/+}$ mice were bred with homozygous CMV-Cre transgenic mice (21) to generate $TIF2^{L-/+}$ mice (mice bearing one allele in which the exon encoding the NID and the selectable marker were deleted), as well as $TIF2^{L2/+}$ mice (mice bearing one "floxed" allele in which the exon encoding the NID is flanked by LoxP sites) (Fig. 1a). Inbreeding of $TIF2^{L-/+}$ mice yielded $TIF2^{L-/L-}$ (also designated as $TIF2^{-/-}$ or TIF2KO) mice homozygous for the deletion of the exon encoding the NID, while inbreeding of $TIF2^{L2/+}$ mice yielded homozygous conditional "floxed" $TIF2^{L2/L2}$ mice.

Mouse genotyping on tail biopsy specimen DNA was performed by PCR using primers P1 (5′-CTGCACGGTGCCAGCAAAGC-3′), P2 (5′-GACCAGGGCT TGCTCAGAAC-3′), and P3 (5′-CCCCTGGATTGTTCCAAAGG-3′) (Fig. 1a; targeted allele). The size of P2-P3 fragment from WT is 289 bp, that of the P1-P3 fragment from the $TIF2^{L-}$ allele is 512 bp, and that of the P2-P3 fragment from the $TIF2^{L2}$ allele is 405 bp (Fig. 1b).

Detection of TIF2 mRNA and protein on tissue sections. Immunofluorescence labeling for detection of TIF2 was performed on 10-μm-thick sections of freshly

frozen testes from 3-month-old WT mice, using a polyclonal antibody raised in rabbit against a peptide corresponding to residues 468 to 481 of GRIP1 (51). The sections were collected on Super Frost Plus coated slides (Kindler, Freiburg, Germany), postfixed with 2% paraformaldehyde in phosphate-buffered saline (PBS) for 4 min at room temperature, washed in PBS containing 0.1% Triton X-100 (PBST) (three times for 3 min), incubated with the primary antiserum (diluted at 10 μm/ml), washed again, and then incubated with Cy3-conjugated anti-rabbit immunoglobulins G (45 min; room temperature; Jackson Immunoresearch). Sections of TIF2$^{-/-}$ testes and incubation of the primary antibody with a 30-fold excess of the immunizing peptide were used as negative immunostaining controls. Sections were counterstained with DAPI (4′,6′-diamidino-2-phenylindole) in Vectashield mounting medium.

In situ hybridization (ISH) was performed on 10-μm-thick sections postfixed in 4% paraformaldehyde in PBS for 30 min at 4°C, washed twice in PBS, and hybridized with a ^{35}S-labeled probe for mTIF2 (nucleotide 1639 to 2500 [accession number U39060]) as described previously (18).

Histological and ultrastructural analyses and detection of proliferating and apoptotic cells in TIF2 mutant testes. For histological analysis, testes of WT and TIF2$^{-/-}$ mice were fixed in Bouin's fluid. Seven-micrometer-thick paraffin sections were stained with hematoxylin and eosin. For ultrastructural studies, mice under deep anesthesia were perfused with 2.5 glutaraldehyde in PBS. The testes were dissected, sliced, and immersed for 16 h at 4°C in the same fixative. After osmium postfixation, dehydration in graded alcohols and embedding in Epon, ultrathin sections (70 nm thick) were contrasted with uranyl acetate and lead citrate.

Detection of apoptotic cells on sections from paraformaldehyde-fixed and paraffin-embedded testes was performed by TdT-mediated dUTP nick-end labeling (TUNEL) according to the manufacturers instructions (in situ cell death detection kit, fluorescein; Roche). To identify proliferating cells, mice received four intraperitoneal injections at intervals of 2 h with 50 mg of bromodeoxyuridine (BrdU)/kg of body weight. Testes were collected 2 h after the last BrdU injection, fixed in 4% paraformaldehyde in PBS (16 h; 4°C). Paraffin sections were incubated with an antibody against BrdU (Boehringer Mannheim) diluted 1/100 in PBS containing 0.1% normal goat serum (16 h; 4°C), revealed with Cy3-conjugated anti-rabbit immunoglobulin G, and mounted in Vectashield medium containing DAPI.

Fertility of TIF2 mutant mice. TIF2-null young females (7 to 10 weeks old) and fertile males (WT) were bred during 4 months. The number of pups per litter and the number of litters per female were scored. Male fertility was similarly tested by breeding TIF2-null young males and WT females.

Superovulation and oocyte quantification. Four-week-old WT and TIF2-null females received intraperitoneal injections with 10 U of PMSG (Folligon-Intervet) followed by 5 U of hCG (Chorulon-Intervet) 48 h later, and sacrificed 19 to 22 h after hCG injection. Oocyte-cumulus masses were extracted from oviducts, and oocytes were counted after enzymatic dissociation from the surrounding cumulus with hyaluronidase (37°C, 1 h) (26).

In vivo fertilization test. After superovulation WT females were mated with TIF2-null males. Females with vaginal plug were sacrificed, oocyte/cumulus masses were extracted from oviducts, and oocytes were counted after enzymatic dissociation from the surrounding cumulus with hyaluronidase. Oocytes were then cultured for 24 h, and the number of fertilized oocytes was scored by counting two blastomere-embryos.

Hormonal treatments. For stimulation of prostate growth, 3-month-old mice were castrated on day 0 and treated with testosterone (3 mg/kg/day) by subcutaneous injection from day 9 to day 15. The total weight of prostate was measured on day 16. Stimulation of uterine growth by estrogen was assessed using ovariectomized 8-week-old females as described previously (39). Uterine wet weight was measured and the ratio of uterine weight to body weight was calculated.

RESULTS

Generation of TIF2-null (TIF2$^{-/-}$) mutant mice. To disrupt mTIF2 (the mouse homolog of human TIF2, also known as GRIP1), we deleted the exon encoding the NID (65; our unpublished results), using the Cre-lox technology and a targeting vector in which three *loxP* sites flank that exon and the TK-neo cassette (Fig. 1a). Complete Cre-mediated excision of the NID sequence in the TIF2 allele L3 generated the allele L$^-$ with a frameshift starting at Arg 375 (mutated in Ser) and extending up to a new stop codon at amino acid position 490 (M. R. Stallcup [sequence accession number U39060]). Thus, the mutated TIF2 allele L$^-$ has the capacity to encode a 489-amino-acid truncated protein, that lacks all TIF2 amino acids C-terminal of the first NID residue. Partial Cre-mediated excision of the TK-neo cassette yielded the conditional floxed TIF2 allele L2 (Fig. 1a).

Chimeric males originating from two independently targeted L3 ES clones (identified by Southern blotting) transmitted the mutation through their germ line (data not shown). To perform the Cre recombinase-mediated excision of the NID, heterozygous TIF2$^{+/L3}$ mice were mated with CMV-Cre mice (21). Inbreeding of the heterozygous TIF2$^{+/L-}$ offspring (identified by PCR [Fig. 1b]) yielded TIF2$^{L-/L-}$ mice. A total of 561 offspring were obtained at the weaning stage from heterozygous parents including 173 TIF2$^{+/+}$ (31%), 288 TIF2$^{+/L-}$ (51%), and 100 TIF2$^{L-/L-}$ (18%) mice. The lower-than-expected percentage of TIF2$^{L-/L-}$ mice was due to death during the first month of their life, as E18.5 fetuses and 5-day-old (P5) newborns were found in a Mendelian distribution (data not shown). The absence of the NID in the putative mutated TIF2 protein was assessed by immunohistochemistry with an antibody recognizing epitope within the WT mouse TIF2/GRIP1 residues 468 and 481 (51). The strong signal observed with this antibody in WT testes was clearly absent in TIF2$^{L-/L-}$ testes (see Fig. 4c to f, and data not shown).

TIF2 deletion results in transient postnatal growth retardation and hypofertility of both sexes. At embryonic day 18.5 (E18.5), the weight of TIF2$^{L-/L}$ (hereafter called TIF2$^{-/-}$) male and female fetuses was not significantly different from that of WT fetuses (data not shown), but 5-day-old (P5) TIF2$^{-/-}$ newborns were ~30% lighter and harmoniously smaller than their WT littermates. This weight deficit and smaller size disappeared progressively after weaning, and by 3 months of age mutant animals were similar to WT (Fig. 2a). Thus, TIF2 appears to be required for normal growth during the suckling period only. This growth deficiency of TIF2$^{-/-}$ mutants is clearly different from that exhibited by p/CIP$^{-/-}$ (SRC3$^{-/-}$) mutants, which has revealed a unique function of p/CIP for regulating normal somatic growth from E13.5 through maturity (66, 72). Sexually mature TIF2$^{-/-}$ males and females were healthy and showed no apparent abnormalities in the major organs at the gross and histological levels (data not shown). However, both males and females were hypofertile.

In continuous mating studies, TIF2$^{-/-}$ females presented normal copulatory plugs, indicating a normal sexual activity, but were hypofertile with reduced numbers of litters and pups per litter (Table 1). Ovarian and uterine functions were analyzed to gain insight into this reduced fertility. The average yield of oocytes collected in the oviduct was similar in superovulated prepubertal TIF2$^{-/-}$, TIF2$^{+/-}$ and WT females, indicating that TIF2 is not required for ovulation (Table 2). Furthermore, estrogen treatment of ovariectomized TIF2$^{-/-}$ and WT females resulted in similar increases in uterine weight, showing that TIF2 is not required to mediate this uterine response (Fig. 2b). Mammary glands from virgin, pregnant, and nursing TIF2$^{-/-}$ females were histologically and functionally normal (data not shown).

Mating TIF2$^{-/-}$ males with WT females generated a number of litters not statistically different from that obtained with

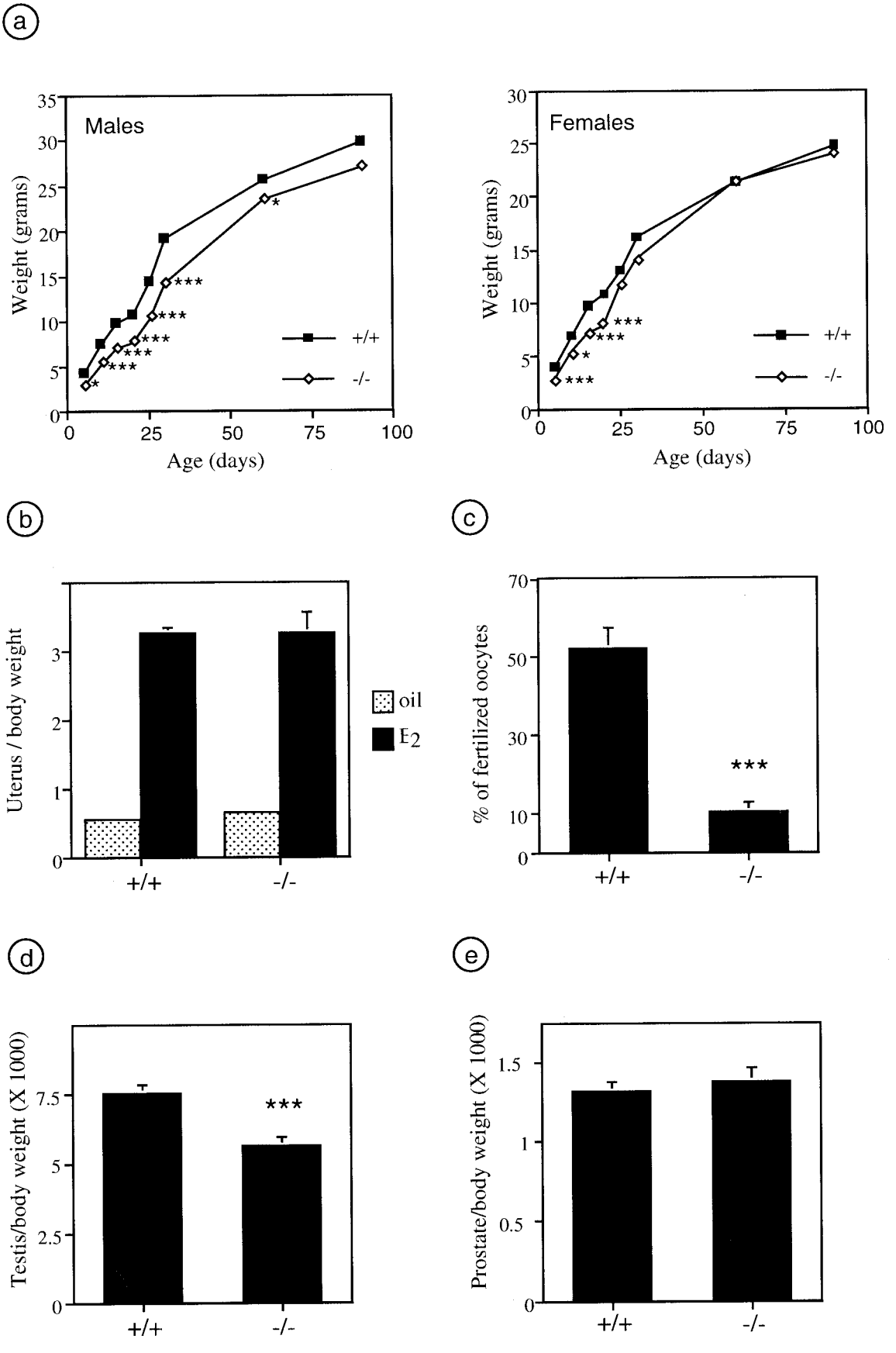
a
Males
Weight (grams)
Age (days)
+/+
-/-
Females
b
Uterus / body weight
oil
E2
+/+
-/-
c
% of fertilized oocytes
d
Testis/body weight (X 1000)
e
Prostate/body weight (X 1000)

TABLE 1. TIF2$^{-/-}$ fertility in continous matings[a]

Gender	Genotype	No. of mice tested	Mean no. of pups/litter ± SD	Mean no. of litters/mouse
Female	WT	4	6.7 ± 1.0	3.5 ± 0.3
	TIF2$^{+/-}$	11	6.1 ± 0.4	3.6 ± 0.3
	TIF2$^{-/-}$	6	2.5 ± 0.3[b]	1.8 ± 0.5[b]
Male	WT	6	7.8 ± 0.4	3.5 ± 0.2
	TIF2$^{+/-}$	10	6.8 ± 0.6	3.4 ± 0.3
	TIF2$^{-/-}$	6	4.6 ± 0.7[b]	2.2 ± 0.7

[a] TIF2 mutant female and male fertility in continuous matings. Control (WT, TIF2$^{+/-}$) and TIF2$^{-/-}$ females (7 to 10 weeks old) or males were bred with males and females, respectively, for 4 months. The number of 3-week-old pups per litter and the number of litter per female were scored.

[b] Level of significance for the observed differences between WT and TIF2$^{-/-}$ mice, $P < 0.05$.

TABLE 2. Ocytes produced after superovulation[a]

Genotype	No. of superovulated females	Oocyte count	
		Avg ± SD	range
WT	9	34.0 ± 3.9	16–51
TIF2$^{+/-}$	11	30.9 ± 3.9	10–61
TIF2$^{-/-}$	10	34.3 ± 4.5	7–65

[a] Oocytes produced after superovulation of prepubertal (4-week-old) WT, TIF2$^{+/-}$, and TIF2$^{-/-}$ females. The responses of WT, TIF2$^{+/-}$, and TIF2$^{-/-}$ females to the superovulation treatment were not statistically different.

WT males. However, the size of these litters was reduced (Table 1), and oocyte fertilization assays carried out in vivo with TIF2$^{-/-}$ males revealed that only 10% of the oocytes were fertilized, compared to 50% with WT males (Fig. 2c). At 3 months of age, the testis weight of TIF2$^{-/-}$ mice was decreased by ~30% relative to that of WT animals (Fig. 2d). However, the size and histology of other testosterone-sensitive organs, such as seminal vesicles and prostate, were normal (data not shown). To further investigate the possible involvement of TIF2 in androgen receptor function, we measured prostate growth in castrated TIF2$^{-/-}$ males upon androgen treatment. Both WT and TIF2$^{-/-}$ males exhibited prostate regression 1 week after castration, and similar prostate-to-body-weight ratios were observed after 7 days of androgen stimulation (Fig. 2e).

Maternal TIF2 is required during pregnancy. A marked increase of in utero embryonic resorptions was observed between E12.5 and E18.5 during pregnancies of TIF2-null dams (Table 3), indicating that the reduced number of pups per litter and litters per dam observed in TIF2$^{-/-}$ females can be accounted for by fetal death. The percentage of embryonic resorptions was not significantly different in WT and TIF2$^{-/-}$ pregnant females at E10.5 but markedly increased at later stages (Table 3). Interestingly, embryos from pregnancies obtained by mating TIF2$^{+/-}$ males with TIF2$^{-/-}$ females, analyzed macroscopically and histologically at E10.5, and compared to those from crosses with TIF2$^{+/-}$ females, appeared smaller and developmentally delayed, irrespective of their genotype (i.e., TIF2$^{+/-}$ or TIF2$^{-/-}$; compare Fig. 3a and b and data not shown). Likewise, the placentas of E10.5 embryos obtained from crosses with TIF2$^{-/-}$ dams often displayed a marked hypoplasia with decreased numbers of trophoblastic trabeculae and embryonic capillaries in the labyrinthine region, resulting in a placenta appearance comparable to that normally observed at E9.5 (Fig. 3c and d and data not shown). Furthermore, this placental hypoplasia occurred irrespective of its genotype (identical to that of the corresponding embryo), and its severity was correlated with the growth retardation of the embryo (data not shown). However, the differentiation status of the trophoblastic lineage was normal as assessed by ISH with molecular probes specific for giant cells (PL-1), spongiotrophoblasts (4311), and labyrinthine trophoblasts (GCM-1) (see references 47 and 68). As TIF2 expression was detected by reverse transcription-PCR analysis in uterine decidua (data not shown), the absence of a maternally derived paracrine signal in TIF2$^{-/-}$ mutant dams could possibly account for the placental abnormalities and subsequent death of the fetuses irrespective of their genotype. However, decidual stroma cells of TIF2$^{-/-}$ mutant appeared histologically normal (data not shown).

TIF2 transcripts and proteins are expressed in Sertoli cells, but not in germ cells. The localization of TIF2 transcripts in the testis seminiferous epithelium of WT males was investigated by ISH with a radioactive cDNA probe. A specific ISH signal was detected in every seminiferous tubule (compare Fig. 4a and b). It was most intense in the peripheral portion of the tubules where most of the Sertoli cell cytoplasm is located. Weaker ISH signals were observed in more luminal portions, where the silver grains often appeared radially aligned, a pattern consistent with a localization in cytoplasmic processes of Sertoli cells (Fig. 4a and data not shown). Immunostaining of WT seminiferous tubules with an anti-TIF2 antibody (51) showed a positive signal only in cell nuclei which, based on their localization at the periphery of the seminiferous tubules (Fig. 4c) and triangular shapes, were identified as Sertoli nuclei

FIG. 2. Postnatal growth, fertility, and hormonal responses of the genital tract in TIF2$^{-/-}$ mutant mice. (a) Weight of male and female TIF2$^{+/+}$ WT (n = 20 and 28, respectively) and TIF2$^{-/-}$ mutant (n = 18 and 11, respectively) mice. Offspring derived from intercrosses between TIF2$^{+/-}$mice were weighed every 5 days during the first month and then were weighed every month from day 30 until 3 months of age. Asterisks indicate the level of significance for the observed differences between WT and TIF2$^{-/-}$ mice (*, $P < 0.05$; and ***, $P < 0.001$). Note that TIF2$^{+/-}$ mice grew at similar rates as their WT littermates (data not shown). (b) Stimulation of uterine growth by estradiol in ovariectomized 8-week-old females. The t test did not reveal any significant difference in the ratio of uterine to body weight between E2-treated WT (n = 8) and TIF2$^{-/-}$ (n = 9) uteri. (c) Capability of TIF2$^{-/-}$ sperm to fertilize oocytes in vivo. Three-month-old males (11 WT and 10 TIF2$^{-/-}$) were mated with superovulated WT (C57/B6) females. Oocytes collected from the oviduct were cultured for 24 h. Fertilized oocytes consisting of two well-formed blastomeres were significantly less frequent in matings involving TIF2$^{-/-}$ males (***, $P < 0.001$ by t test). (d) Smaller testes in TIF2$^{-/-}$ mutants. The testis and the body weight were measured in 3-month-old mice (23 TIF2$^{-/-}$ mice and 22 WT mice). The ratio of testis weight to body weight was significantly decreased in TIF2$^{-/-}$ males (***, $P < 0.001$ by t test). (e) Stimulation of prostate growth by testosterone. Three-month-old mice (13 TIF2$^{-/-}$ mice and 14 WT mice) were castrated and then treated with testosterone. The t test did not reveal any significant difference.

TABLE 3. Embryonic resorptions in WT and TIF2$^{-/-}$ mice[a]

Female genotype	Result on:															
	E10.5				E12.5				E14.5				E18.5			
	n(l)	n(e)	n(r)	% *r*	n(l)	n(e)	n(r)	% *r*	n(l)	n(e)	n(r)	% *r*	n(l)	n(e)	n(r)	% *r*
WT	8	67	1	1.5	4	42	4	9.5	6	51	3	5.9	5	51	5	9.8
TIF2$^{-/-}$	7	56	2	3.6	6	42	14	33.3	2	19	14	73.7	2	17	7	41.2

[a] Embryonic resorptions in WT and TIF2$^{-/-}$ female, from E10.5 to E18.5. Abbreviations: *n*(*l*), number of litters; *n*(*e*), total number of embryos; *n*(*r*), number of resorptions; % *r*, % embryonic resorptions per litter.

(Fig. 4c and e). Germ cells—e.g., spermatocytes (Fig. 4e), round spermatids, and elongated spermatids—were not immunostained (Fig. 4 e). Moreover, TIF2 transcripts and proteins were absent from both myoepithelial cells that surround the seminiferous epithelium (Fig. 4e) and Leydig cells (Fig. 4a, c, and e). No labeling was ever detected when the antibody was preincubated with an excess of the immunizing peptide (Fig. 4d) nor in TIF2$^{-/-}$ seminiferous epithelium (Fig. 4f). Thus, TIF2 testicular expression is restricted to Sertoli cell nuclei and does not depend on the stage of the seminiferous epithelium cycle.

Defects in spermiogenesis account for the hypofertility syndrome. The hypofertility syndrome of 3-month-old TIF2$^{-/-}$ males was clearly not due to testicular degeneration nor to a

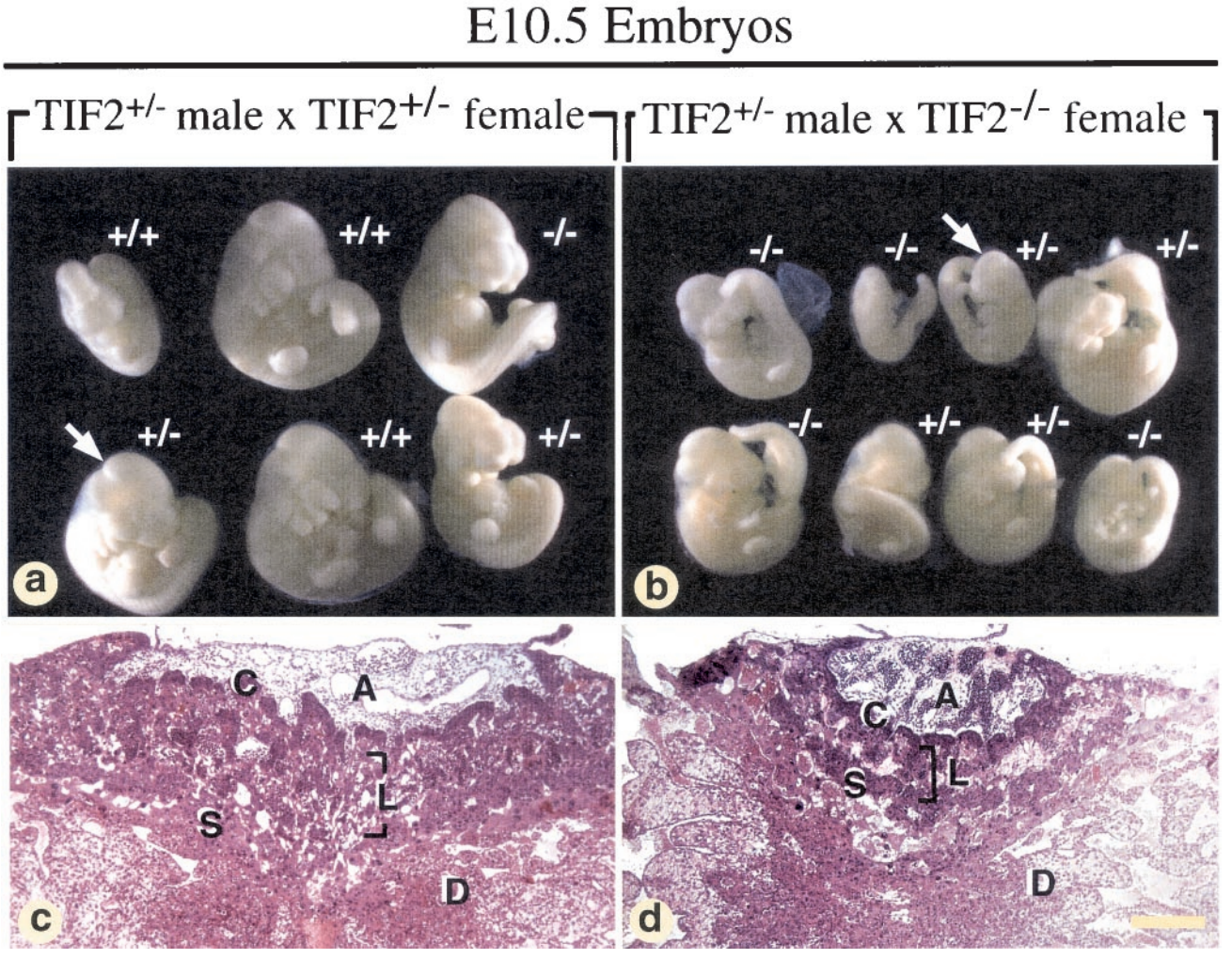

FIG. 3. External views of litters (a and b) and histological sections of placentas (c and d) from TIF2$^{+/-}$ (a and c) and TIF2$^{-/-}$ (b and d) pregnancies at E10.5. The placenta comprises (i) a chorionic plate (C), which is traversed by allantoic capillaries; (ii) a labyrinthine region (L) composed of strands of trophoblast cells and of a network of extraembryonic capillaries, interspersed with maternal blood sinuses; (iii) a spongiotrophoblast (S), in which only maternal blood circulates. The arrows in panels a and b point to the embryos whose placentas are displayed in panels c and d, respectively. Other abbreviations: A, allantois; D, uterine deciduae. Bar: 100 μm.

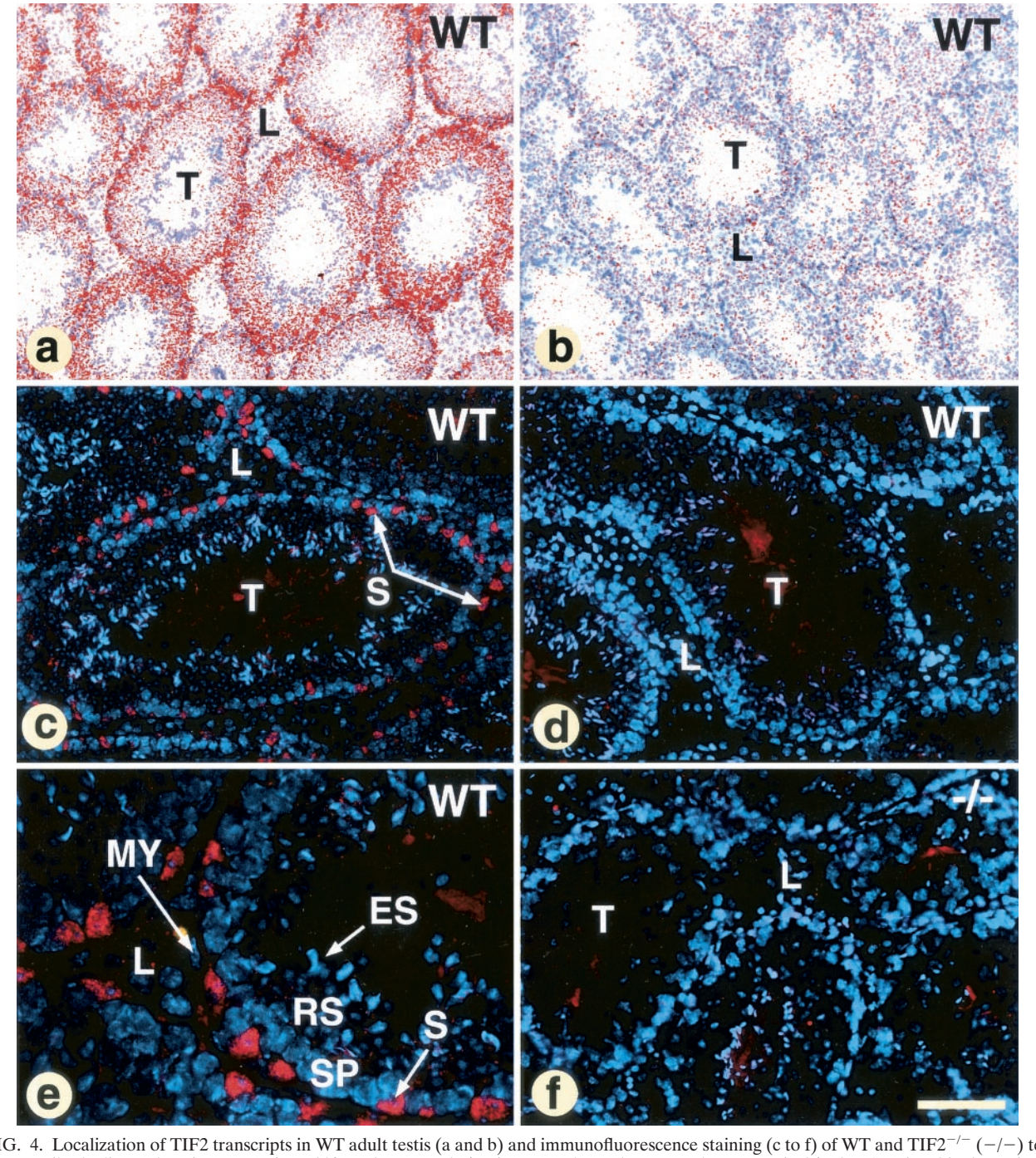

FIG. 4. Localization of TIF2 transcripts in WT adult testis (a and b) and immunofluorescence staining (c to f) of WT and TIF2$^{-/-}$ ($-/-$) testes with an antibody directed against TIF2. (a and b) In these panels (antisense probe and sense probe, respectively), the ISH signal is shown in false colors after computer processing of a bright-field view and dark-field view of the same section. TIF2 transcripts are present in every seminiferous tubule and are more abundant at the periphery of the tubules. A strong positive immunofluorescence signal is specifically detected in WT, but not in TIF2$^{-/-}$ Sertoli cells (compare panels c and e with panel f). This signal is not seen in WT cells after preincubation of the antiserum with the immunizing peptide (d), and absent from WT germ line, peritubular, myoepithelial (MY) and Leydig (L) cells. Other abbreviations: ES, elongated spermatids; RS, round spermatids; S, Sertoli cells; SP, spermatocytes; T, seminiferous tubules. The bar in panel f represents 100 μm (a and b), 40 μm (c, d, and f), and 15 μm (e).

decrease in the production spermatozoa. Indeed, with two exceptions (see below), their testes (n = 14) were indistinguishable from those of their WT counterparts on both paraffin and Epon (semithin) sections (Fig. 5a and b and data not shown), and the concentrations of spermatozoa in fluid from caudal epidydimides were similar in TIF2$^{-/-}$ (n = 6) and WT males (data not shown).

In histologically normal testes from 3-month-old TIF2$^{-/-}$

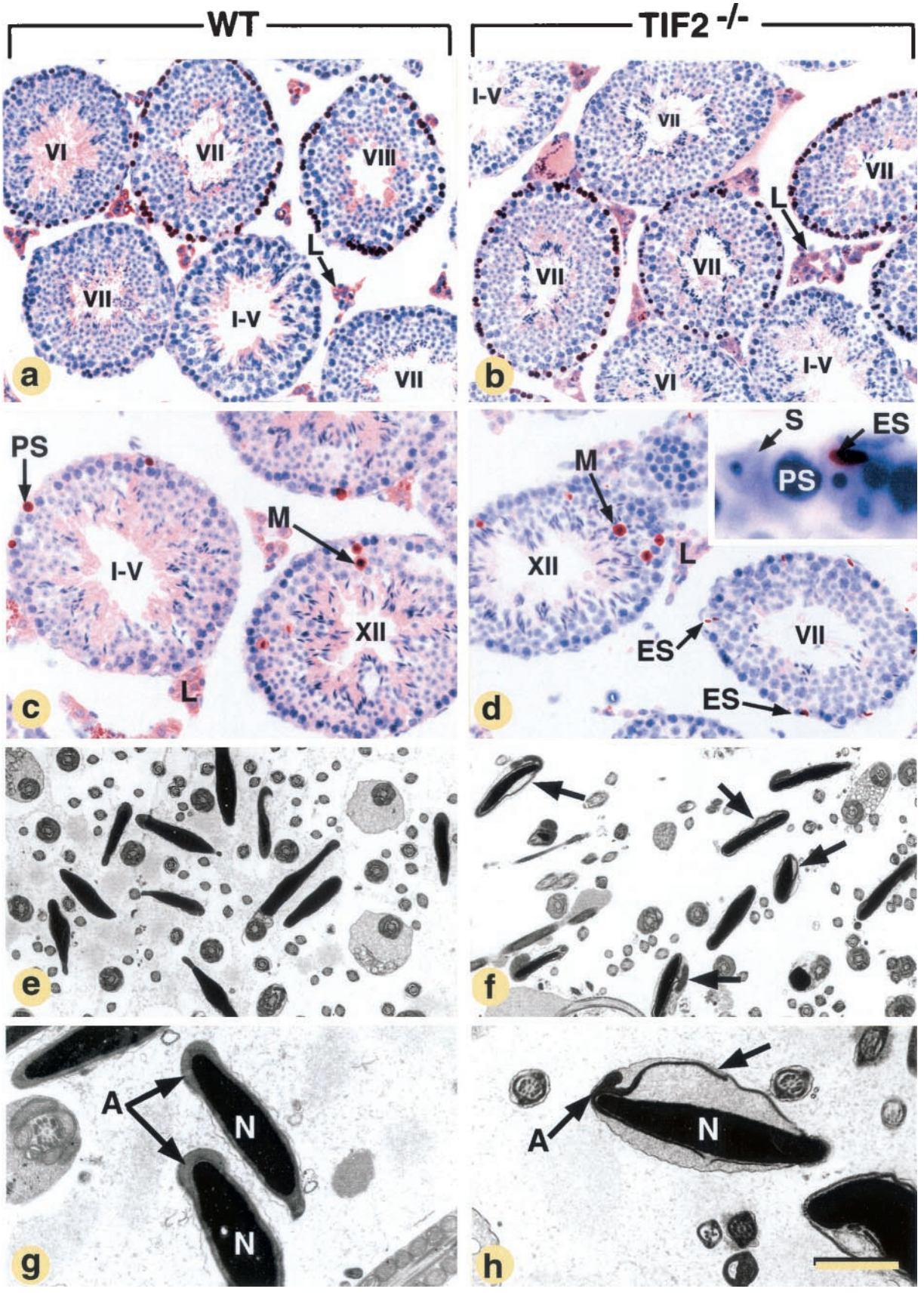
WT
TIF2 -/-
VI
VII
VIII
L
VII
I-V
VII
a
I-V
VII
VII
L
VII
VII
VI
I-V
b
PS
M
I-V
XII
L
c
M
XII
L
S
ES
PS
ES
VII
ES
d
e
f
A
N
N
g
A
N
h

mutants, the pattern of cell proliferation, as assessed by BrdU incorporation into S-phase nuclei, was not altered: in both WT and TIF2$^{-/-}$ testes, ~65% of the tubules at stage VII of the seminiferous epithelium cycle displayed BrdU-labeled preleptotene spermatocytes (brown pseudocolor in Fig. 5a and b); labeled type B spermatogonia were numerous in stage VI tubules and scarce in stage II to stage V tubules; tubules at stages IX-XII were always devoid of labeling by BrdU, as well as nuclei of type A and other early proliferating spermatogonia (Fig. 5a and b and data not shown; 19). Apoptotic cell death assessed by TUNEL assays occurred essentially during metaphase I (Fig. 5c and d) and to a lesser extent in pachytene spermatocytes (PS) (35), and was similar in 3-month-old WT and mutant testes (Fig. 5c and d, and data not shown). Therefore, it appears unlikely that defects in germ cell proliferation or survival account for the hypofertility of TIF2$^{-/-}$ males. On the other hand, degenerating, TUNEL-positive elongate spermatids were seen at the periphery of some TIF2$^{-/-}$ seminiferous tubules (Fig. 5d) but not in WT counterparts. As it is well established that abnormal elongate spermatids are often phagocytosed by Sertoli cells instead of being released into the tubular lumen (56), we studied the morphology of epididymal spermatozoa.

The percentage of abnormal spermatozoa in smears from epididymal fluid was twofold increased in TIF2$^{-/-}$males (37% of spermatozoa with bent tails and necks versus 16% in WT males) (data not shown). At the electron microscopic level, many acrosomes (about 70%) were partially detached from the nuclear envelope (compare Fig. 5f and 5e; also compare A in Fig. 5g and h), thus strongly suggesting impaired attachment of the acrosomal membrane to the nucleus in TIF2$^{-/-}$ mutants. Spermatozoa mitochondria appeared normal. Thus, teratozoospermia (i.e., frequent abnormalities of spermatozoa in the semen) is, at least in part, responsible for hypofertility of 3 month-old TIF2$^{-/-}$ males.

TIF2$^{-/-}$ mutants display an age-dependent testicular degeneration. The histological appearance of the testis was markedly altered in 2 (out of 14) and 1 (out of 4) TIF2$^{-/-}$ males analyzed at 3 and 6 months of age, respectively, as well as in all TIF2-null mutants examined at 9 months ($n = 2$), 12 months ($n = 3$), and 20 months ($n = 2$) of age. Thus, the degeneration of TIF2$^{-/-}$ testes has a highly variable onset but becomes completely penetrant by 9 months of age. In these TIF2$^{-/-}$ degenerating testes, the diameter of the seminiferous tubules was decreased, some of these tubules were devoid of a lumen (Fig. 6a, b, g, and h), and frequently displayed large intercellular vacuoles (Fig. 6b and 7b) and absence of spermatids.

A variable percentage (5 to 70%, depending on the animal) of tubular cross-sections contained either TUNEL-positive mutinucleate giant cells (i.e., symplasts [Fig. 6c and 7a to c]) or large sacs of eosinophilic cytoplasm filled with TUNEL-positive fragments (Fig. 7d and data not shown). The symplasts and the sacs represent dying syncytia formed from spermatocytes (Fig. 7a), round and elongated spermatids (Fig. 6c and 7b and c), through opening of intercellular bridges that normally connect these cells (56). Sloughing off of round spermatids was observed in many seminiferous tubules (Fig. 6c), and Sertoli cell-only tubules were occasionally present (data not shown). In the rete testis (the intratesticular portion of the genital duct) and epididymis from mutant mice, the number of immature germ cells was markedly increased; eventually, the mutant genital ducts contained only degenerating round spermatids (Fig. 6d and f) and symplasts (Fig. 6d), instead of spermatozoa (Fig. 6e).

The occurrence of symplasts and shedding of immature germ cells in TIF2$^{-/-}$ tubules strongly suggest that TIF2 expression in Sertoli cells is essential for their adhesion to germ cells. On the other hand, TIF2 does not appear to be critically involved in germ cell proliferation, as spermatogonia and preleptotene spermatocytes showed efficient BrdU incorporation within degenerating tubules (Fig. 7e). Taken together, these observations indicate that TIF2$^{-/-}$ testes suffer from defects in spermiogenesis (spermatid maturation) and spermiation (spermatid release), which are both worsening with age.

TIF2$^{-/-}$ Sertoli cells show increased amounts of intracellular lipids. The cytoplasm at the basal portion of a normal Sertoli cell contains small lipid droplets which, on semithin sections, appear in the form of small osmiophilic inclusions (Fig. 6g) (see reference 34 and references therein). The distribution and size of lipid droplets in TIF2$^{-/-}$ mutant testes were normal at 3 months of age ($n = 4$; data not shown). In contrast, testes from 6-, 9-, and 12-month-old mutants all displayed enlarged Sertoli cell lipid droplets (arrows in Fig. 6 h and i), whose size and number varied greatly between animals (data not shown). Note that Sertoli cell mitochondria did not exhibit any obvious electron microscopy abnormality (data not shown). Such large lipid droplets were observed both in tubules exhibiting signs of degeneration, and in those with normal germ cell associations (Fig. 6i), indicating that lipid accumulation in TIF2$^{-/-}$ Sertoli cells is not due to an increase of their phagocytic activity, secondary to germ cell degeneration.

FIG. 5. Detection of proliferating (a and b) and apoptotic cells (c and d) in the testes and electron microscopic analysis of the epididymides (e to h) in WT and histologically normal TIF2$^{-/-}$ mice at 3 months of age. Abbreviations: A, acrosome; ES, elongated spermatids; L, Leydig cells; M, spermatocytes in metaphase; N, nuclei of spermatozoa; PS, pachytene spermatocytes; S, Sertoli cells; T, seminiferous tubules. Roman numerals refer to stages of the seminiferous epithelium cycle (Russell et al. [56]). Each stage is defined by a specific association of germ cell types, and the cycle corresponds to the series of change occurring at a given level of the seminiferous tubule between two successive appearances of the same cell association. In normal mice, there are 12 stages, designated I to XII. (a and b) A brown pseudocolor was assigned to BrdU-labeled cells, and a blue pseudocolor was assigned to the DAPI nuclear counterstain; the brown signal in Leydig cells is purely cytoplasmic and corresponds to unspecific binding of the antibody to the histological section. (c and d) The brown signal corresponds to nuclei containing DNA fragments. The inset (d) shows a high magnification of a TUNEL-positive elongate spermatid localized at the periphery of a seminiferous tubule. (f, g, and h) Arrows point to acrosomes detached from the nuclear envelope. The bar in panel h represents 160 μm (a and b), 100 μm (c and d), 11 μm (e and f), and 4 μm (g and h).

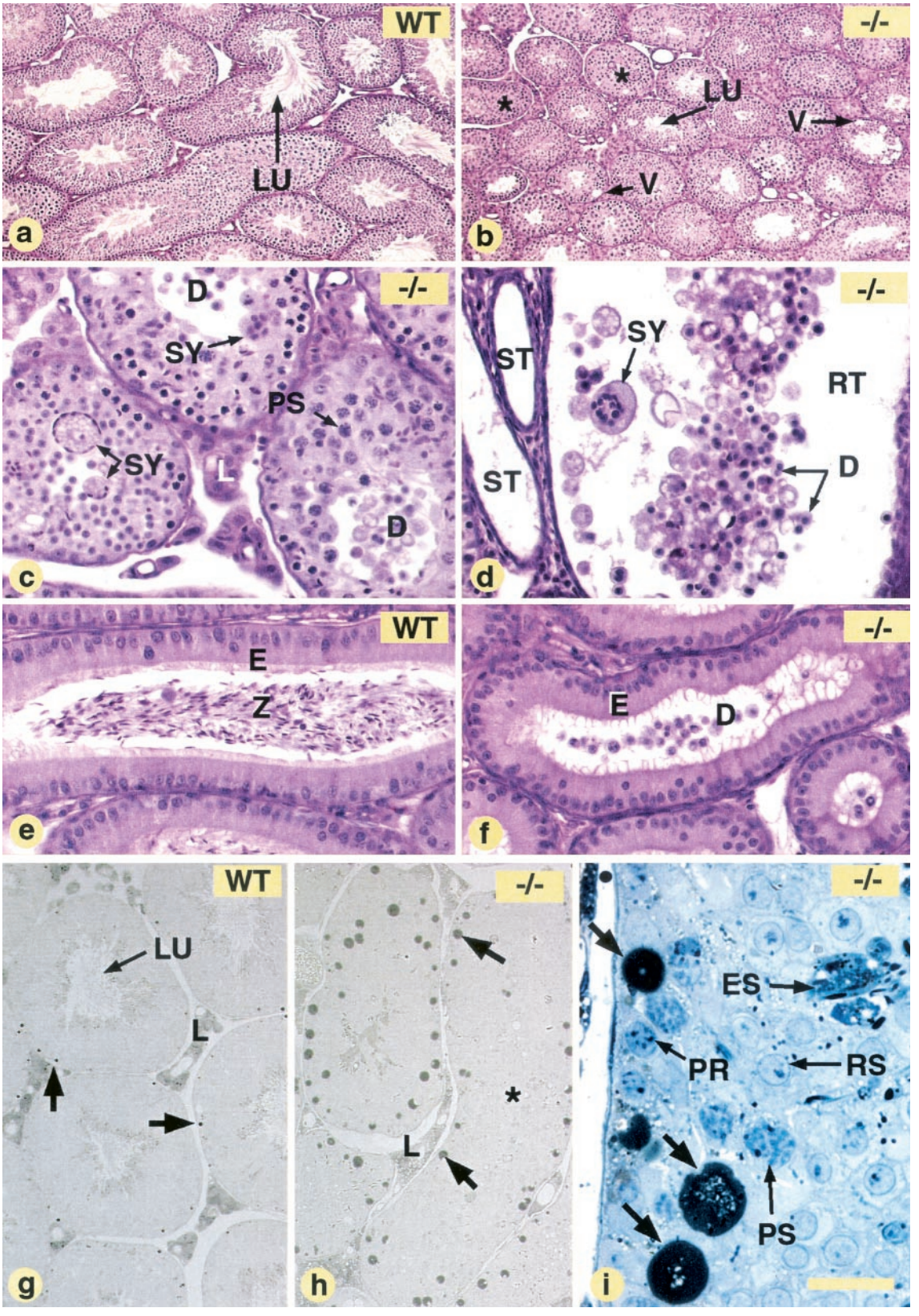

FIG. 6. Release of immature spermatids and lipid droplet accumulation in TIF2$^{-/-}$ mutants. (a to i) Comparison of the testes and epididymides from WT and TIF2$^{-/-}$ ($^{-/-}$) mutants at 12 months (those in panels b, c, d, f, and h are from the same mutant). The asterisks indicate seminiferous tubules lacking a lumen, and arrows point to lipid droplets. Paraffin sections stained with hematoxylin and eosin (a to f), and Epon sections are stained with osmium tetroxide only (g and h) or osmium tetroxide and toluidine blue (i). Abbreviations: D, desquamating round spermatids; E, epithelium of the cranial portion of the epididymis; ES, elongated spermatids; L, Leydig cells; LU, lumen of the seminiferous tubules; PR, preleptotene spermatocytes; PS, pachytene spermatocytes; RS, round spermatids; RT, rete testis; SY, symblasts; ST, straight tubules; V, intercellular vacuoles; Z, spermatozoa. The bar in panel i represents 160 μm (a and b), 40 μm (c to f), 80 μm (g and h) and 15 μm (i).

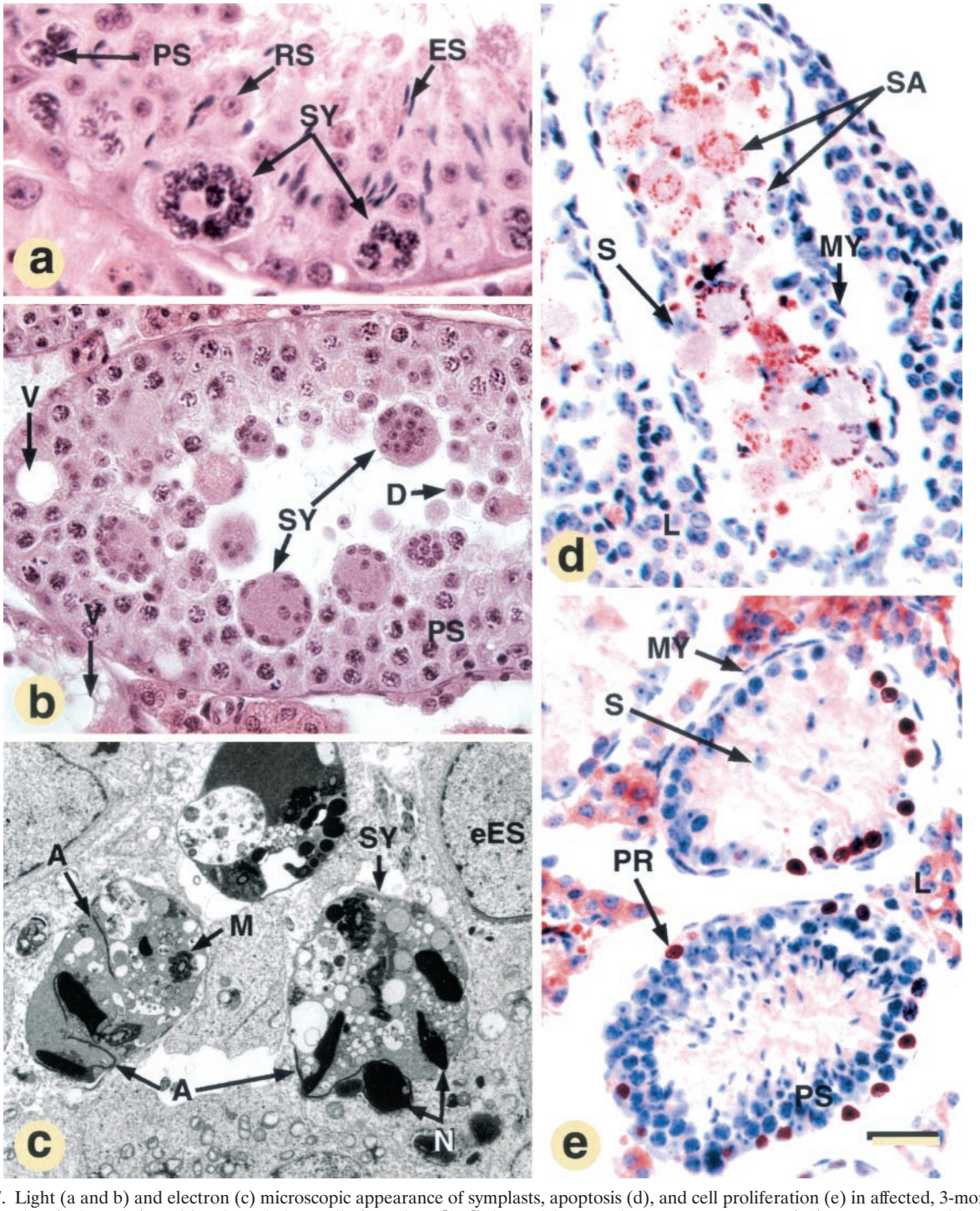

FIG. 7. Light (a and b) and electron (c) microscopic appearance of symplasts, apoptosis (d), and cell proliferation (e) in affected, 3-month-old, $TIF2^{-/-}$ males. (a, b, and c) Multinucleated giant cells (symplasts [SY]) formed from pachytene spermatocytes (PS), round spermatids (RS), or elongated and condensed (ES) spermatids, respectively; note that spermatid-derived symplasts are, by far, the most frequent. (d) TUNEL staining. (e) BrdU incorporation into preleptotene spermatocytes (PR) within degenerated seminiferous tubules lacking round spermatids. The signal in Leydig cell cytoplasm is artifactual (see the legend to Fig. 5). Other abbreviations: A, acrosomes; D, desquamating spermatids; eES, early elongating spermatids; L, Leydig cells; M, mitochondrial sheath; MY, myoepithelial cells; N, nuclei of elongated spermatids; S, Sertoli cell; SA, cytoplasmic sac derived from symplast; SP, spermatocytes; V, vacuoles. The bar in panel e represents 15 μm (a), 40 μm (b, d, and e), and 3 μm (c).

DISCUSSION

To reveal the physiological functions of the NR coactivator TIF2/GRIP1 and to investigate to which extent these functions are distinct from those of the two other members (SRC-1 and p/CIP) of the p160 coactivator family, we have disrupted the TIF2 gene in the mouse. The mutation, which deletes the exon encoding the NID, effectively interrupts the synthesis of the TIF2 protein C-terminal to the first residue of the NID. We cannot rule out the possibility that a truncated protein containing the N-terminal basic helix-loop-helix (bHLH)-PAS domain could still be produced. Nevertheless, several lines of evidence indicate that the present TIF2 gene disruption is a null mutation, as it has been shown that such a bHLH-PAS domain-containing truncated protein (i) cannot bind NRs and has lost its NR coactivation function (8, 65), (ii) is unlikely to exert a dominant negative effect on other p160 family members (73), and (iii) is also unlikely to exert dominant negative effects on other transcription factors that possess a bHLH domain (e.g., Hand1 [52], Mash2 [25], and Arnt [2, 36]); indeed, these genes play important roles in placenta development, but their disruptions result in defects which are different form those generated by TIF2 disruption, and furthermore are not of maternal origin, in contrast to those resulting from the TIF2 mutation. Finally, the lack of defects in TIF2$^{+/-}$ heterozygotes also supports the conclusion that the present TIF2 gene disruption effectively results in a null mutation.

In the present study, we have focused on the role played by TIF2 in mouse reproductive functions. We discuss below these functions that are distinct from those of the two other members of the p160 coactivator family.

Maternal expression of TIF2 is essential for placentation. SRC-1$^{-/-}$ mutant females are fertile and suffer from a partial resistance to steroid hormones that affects uterus and mammary glands (73), whereas p/CIP$^{-/-}$ (SRC-3$^{-/-}$) females exhibit delayed puberty, mammary gland growth retardation, and decreased reproductive function (i.e., defects in ovulatory capacity, litter size, and length of estrous cycle) related to estrogen insufficiency (72). Note, however, that these p/CIP reproductive defects have not been found in a distinct p/CIP null mutant line (66).

Interestingly, none of the SRC-1$^{-/-}$ or p/CIP$^{-/-}$ mutant defects are exhibited by TIF2$^{-/-}$ mutants, as TIF2 is not required for ovulation, fecundation, and implantation, and the impaired reproductive capacity of TIF2$^{-/-}$ females is accounted for by a poor, apparently delayed, development of the chorioallantoic placenta. In litters from TIF2$^{-/-}$ females, this placental hypoplasia most probably accounts for embryonic growth retardation at E10.5 and embryonic lethality between E10.5 and E12.5.

The placenta is a vital organ without which mammalian embryos cannot survive (55) and whose development is influenced by uterine and systemic maternal environments (4). None of the placenta defects exhibited by a number of NR null mutants (6, 42, 57, 68) are similar to those seen in TIF2$^{-/-}$ females, which are therefore unlikely to reflect the impairment of NR signaling pathway(s). As TIF2 is expressed in maternal decidual stromal cells, TIF2$^{-/-}$ placental hypoplasia may reflect some functional defects in these cells. In this respect, we note that TIF2 may act as a coactivator for transcription factors TEF-1, TEF-3 and TEF-5 that belong to the TEF family and are expressed in maternal decidua facing the developing mouse placenta (30). The NR coactivator p160 proteins could indeed be bona fide coactivators of TEF transcription factors, through interaction mediated by their N-terminal bHLH-PAS domain (8).

Whether the partial penetrance of the placental hypoplasia in TIF2$^{-/-}$ dams may reflect a partial functional redundancy between the p160 coactivators will require the analysis of TIF2/SRC-1 and TIF2/p/CIP compound mutants. In any event, and irrespective of the underlying molecular mechanism, our present study suggests that a spectrum of outcomes, including miscarriage and intrauterine growth restriction could arise from mutations of human TIF2.

TIF2 expression in Sertoli cells plays essential roles in fertility and maintenance of the seminiferous epithelium. In contrast to SRC-1$^{-/-}$ and p/CIP$^{-/-}$ (SRC-3$^{-/-}$) mutants (66, 73), TIF2$^{-/-}$ males are hypofertile and exhibit testis abnormalities. Spermatogenesis is critically dependent on intimate contacts and paracrine interactions between Sertoli cells and germ cells. Sertoli cells drive germ cells throughout their development and notably assist the maturation and release of spermatids (24, 56, 59). In turn, spermatocytes and spermatids can influence Sertoli cell gene expression and functions, including lipid storage (10, 23, 31, 60, 71, 75). We have shown here that TIF2 expression is apparently confined to Sertoli cells, which thus represent the main, and perhaps the sole, primary target of TIF2 function in the testis and have demonstrated that TIF2 is essential for efficient spermatogenesis.

Decreased fertility of 3-month-old TIF2$^{-/-}$ males is associated with defects related to spermiogenic impairments: (i) defect of the acrosome, a structure indispensable for fertilization (1); (ii) bendings of necks and tails of spermatozoa, known to cause poor motility (see reference 63 and references therein); and (iii) failure of sperm release manifested by an exacerbation of phagocytosis of mature round spermatids. Together the first two defects are the probable causes of decreased fertility of TIF2$^{-/-}$ males, although taken individually they are not penetrant enough to cause hypofertility (56). The third abnormality does not induce any significant reduction in the number of epididymal spermatozoa. Therefore, teratozoospermia (abnormal sperm morphology) most probably accounts on its own for the decreased fertilization potency of sperm of 3- to 4-month-old TIF2$^{-/-}$ mutants. It is noteworthy that the more severe spermiogenic impairments that cause sterility of RXRβ$^{-/-}$ mutants lead to oligo-astheno-teratozoospermia (34).

Testicular degeneration in older TIF2$^{-/-}$ males is manifested by (i) vacuolation of the seminiferous epithelium, (ii) detachment of spermatocytes and spermatids from the seminiferous epithelium, and (iii) formation of apoptotic, spermatocyte- and spermatid-derived, multinucleate giant cells (i.e., symplasts). The presence of large vacuoles between Sertoli cells, a common feature in testicular degeneration syndromes, is interpreted either a cause or a consequence of germ cell sloughing (48, 56). The last two abnormalities probably reflect disruption of cell adhesion processes between Sertoli cells and germ cells. It is also noteworthy that apoptosis within TIF2$^{-/-}$ testes is not the cause of the observed loss of germ cells, as it does not increase prior to the onset of degeneration.

Thus, our present data strongly suggest that TIF2 is required

in Sertoli cells for short-range cellular interactions with germ cells. That the onset of the testicular degeneration is subject to individual variations, and that this defect becomes progressively more penetrant upon aging, may reflect a functional redundancy between TIF2 and other NR coactivators. Compound mutants (e.g., TIF2/SRC-1 or TIF2/p/CIP) are required to further investigate this possibility. Note in this respect that we have not observed any significant compensatory increase in SRC-1 transcripts in TIF2$^{-/-}$ testis, nor in any other tissues of TIF2$^{-/-}$ mutant that we have analyzed (e.g., lung, ovary, uterus, liver, and brain). Finally, our data obviously suggest that TIF2 mutations could be involved in some case of human male hypofertility or sterility.

Lipid metabolism defect in Sertoli cells of TIF2 null mutants. It is often assumed that lipid droplets in the basal cytoplasm of Sertoli cells arise from the incomplete degradation of immature germ cells (56, 58). The occurrence of large lipid droplets within Sertoli cells has been described in several pathological conditions associated with chronic germ cell degeneration, such as combined radio- and chemotherapy, exposure to high concentrations of estrogens, as well as testicular aging (58). However, there exist other situations, as for example vitamin A deficiency (28) or retinoic acid receptor alpha (RARα) elimination (41), in which testicular degeneration can occur without lipid increase in Sertoli cells. On the other hand, our present data show that, from 3 months of age, TIF2$^{-/-}$ testes can exhibit large lipid droplets in seminiferous tubules in the absence of any sign of degeneration. Most interestingly, similar lipid droplets that are not temporally correlated with the subsequent appearance of testis degeneration are present in seminiferous tubules of RXRβ-null mutants (34). However, in the latter case, these droplets arise earlier at the prepubertal stage and are larger at later stages. Taken together, these observations indicate that lipid accumulation is not a necessary correlate of impaired spermiation and therefore that, similar to the RXRβ-null mutant case, the larger lipid droplets observed in Sertoli cells of TIF2$^{-/-}$mutants reflects a cell-autonomous function(s) of TIF2 in lipid metabolism.

Which signaling pathway(s) is affected in TIF2$^{-/-}$ testis? Sertoli cells express a number of NRs which are potentially capable of functionally interacting with TIF2, including TRα (13), RARα (41; our unpublished results), RXRβ (34) and PPARs (12). TRα-null males are not sterile, but TRα is thought to play an important role in prepubertal testicular growth by controlling the rate of Sertoli cell division (43, 50), and this could also be the case for TIF2, as TIF2-null mutant testes are smaller than those of their WT counterparts. Compound mutants between TIF2 and TRα are required to investigate whether some functional redundancy could mask possible roles of TRα in the spermiogenic defects exhibited by TIF2 null mutants. The testicular phenotype of RARα null mutants matches closely lesions resulting from vitamin A deficiency (41) and is clearly different from the TIF2$^{-/-}$ null defects, as testicular degeneration occurs at much earlier stages in RARα mutants before completion of puberty. Whether this temporal difference in the appearance of spermiogenic defects in RARα$^{-/-}$ and TIF2$^{-/-}$ mutants could also reflect some functional redundancies will again require the examination of compound mutants (e.g., RARα/TIF2 and TIF2/SRC-1).

As already mentioned the defects that characterize the TIF2$^{-/-}$ testis phenotype (accumulation of lipid droplets, degeneration of seminiferous tubules) are very similar to those exhibited by RXRβ$^{-/-}$ mutants, the only difference concerning their time of appearance (note that RXRβ is also expressed in Sertoli cells, but apparently not in germ cells [34]). In the case of RXRβ-null mutants, as in the case of TIF2$^{-/-}$ mutants, lipid accumulation is clearly preceding the degeneration of seminiferous tubule epithelium. Moreover, a mutation that inactivates the AF-2 activation function of RXRβ (RXRβAF2^{0}) is sufficient to induce the accumulation of lipid droplets, whereas full elimination of RXRβ is required to cause the degeneration of seminiferous tubules (B. Mascrez and P. Chambon, unpublished results). It follows that accumulation of lipid droplets, and therefore alteration of lipid metabolism, is apparently not a necessary or a sufficient condition for the generation of defects that lead to seminiferous tubules degeneration. Thus, TIF2 appears to be involved in two processes in the testis: one of them, which involves TIF2 in a cell-autonomous manner, is related to intra-Sertoli cell lipid metabolism and may be mediated by a PPAR/RXRβ heterodimer (12, 34), whereas the other, which involves TIF2 in a cell nonautonomous manner, is related to the function of Sertoli cells in maintenance of the seminiferous epithelium. Future genetic dissection requiring spatio-temporally controlled somatic mutagenesis (45) and compound RXRβ/TIF2 mutants, among others, is necessary to investigate whether the variable penetrance of the TIF2 and RXRβ mutations on testis phenotype reflects functional redundancies between the p160 coactivators, as well as between RXR isotypes.

In conclusion, our present data indicate that TIF2 plays an important role(s) in the control of spermatogenesis, as well as in Sertoli cell metabolism, most probably through signaling pathways that involve several NRs. More generally, our present genetic dissection study further demonstrates that the three members of the p160 NR coactivator family actually play distinct physiological functions, even though they may exhibit some functional redundancy.

ACKNOWLEDGMENTS

Martine Gehin and Manuel Mark contributed equally to this study.

We gratefully acknowledge T. Ylikomi for the gift of TIF2 antibody. We also thank P. Dollé for helpful discussion; B.Chapellier and J.-M. Garnier for TIF2 genomic cloning; A. Gansmuller for electron microscopy; and V. Fraulob, G. Gasnier, C. Hummel, I. Tilly, and B. Weber for their technical help.

This work was supported by funds from the Centre National de la Recherche Scientifique (CNRS), the Institut National de la Santé et de la Recherche Médicale (INSERM), the Hôpital Universitaire de Strasbourg, the Collège de France, the Institut Universitaire de France, the Association pour la Recherche sur le Cancer (ARC), the Fondation pour la Recherche Médicale (FRM), the Ligue Nationale contre le Cancer, the European Community (QLG3-CT2000-00844), the Human Frontier Science Program, and Bristol-Myers Squibb.

REFERENCES

1. **Abou-Haila, A., and D. R. Tulsiani.** 2000. Mammalian sperm acrosome: formation, contents, and function. Arch. Biochem. Biophys. **379:**173–182.
2. **Adelman, D. M., M. Gertsenstein, A. Nagy, M. C. Simon, and E. Maltepe.** 2000. Placental cell fates are regulated in vivo by HIF-mediated hypoxia responses. Genes Dev. **14:**3191–3203.
3. **Anzick, S. L., J. Kononen, R. L. Walker, D. O. Azorsa, M. M. Tanner, X. Y. Guan, G. Sauter, O. P. Kallioniemi, J. M. Trent, and P. S. Meltzer.** 1997. AIB1, a steroid receptor coactivator amplified in breast and ovarian cancer. Science **277:**965–968.
4. **Aplin, J.** 2000. Maternal influences on placental development. Semin. Cell Dev. Biol. **11:**115–125.

5. **Bannister, A. J., and T. Kouzarides.** 1996. The CBP co-activator is a histone acetyltransferase. Nature **384:**641–643.
6. **Barak, Y., M. C. Nelson, E. S. Ong, Y. Z. Jones, P. K. Ruiz-Lozano, R. Chien, A. Koder, and R. M. Evans.** 1999. PPAR gamma is required for placental, cardiac, and adipose tissue development. Mol. Cell **4:**585–595.
7. **Bautista, S., H. Valles, R. L. Walker, S. Anzick, R. Zeillinger, P. Meltzer, and C. Theillet.** 1998. In breast cancer, amplification of the steroid receptor coactivator gene AIB1 is correlated with estrogen and progesterone receptor positivity. Clin. Cancer Res. **4:**2925–2929.
8. **Belandia, B., and M. G. Parker.** 2000. Functional interaction between the p160 coactivator proteins and the transcriptional enhancer factor family of transcription factors. J. Biol. Chem. **275:**30801–30805.
9. **Blanco, J. C., S. Minucci, J. Lu, X. Yang, J. K. K. Walker, H. Chen, R. M. Evans, Y. Nakatani, and K. Ozato.** 1998. The histone acetylase PCAF is a nuclear receptor coactivator. Genes Dev. **12:**1638–1651.
10. **Boujrad, N., M. T. Hochereau-de Reviers, and S. Carreau.** 1995. Evidence for germ cell control of Sertoli cell function in three models of germ cell depletion in adult rat. Biol. Reprod. **53:**1345–1352.
11. **Bourguet, W., P. Germain, and H. Gronemeyer.** 2000. Nuclear receptor ligand-binding domains: three-dimensional structures, molecular interactions and pharmacological implications. Trends Pharmacol. Sci. **21:**381–388.
12. **Braissant, O., F. Foufelle, C. Scotto, M. Dauça, and W. Wahli.** 1996. Differential expression of peroxisome proliferator-activated receptors (PPARs): tissue distribution of PPAR-α, -β, and -γ in the adult rat. Endocrinology **137:**354–366.
13. **Buzzard, J. J., J. R. Morrison, M.K. O'Bryan, Q. Song, and N. G. Wreford.** 2000. Developmental expression of thyroid hormone receptors in the rat testis. Biol. Reprod. **62:**664–669.
14. **Carapeti, M., R. C. Aguiar, J. M. Goldman, and N. C. Cross.** 1998. A novel fusion between MOZ and the nuclear receptor coactivator TIF2 in acute myeloid leukemia. Blood **91:**3127–3133.
15. **Champagne, N., N. Pelletier, and X. J. Yang.** 2001. The monocytic leukemia zinc finger protein MOZ is a histone acetyltransferase. Oncogene **20:**404–409.
16. **Chen, D., H. Ma, H. Hong, S. S. Koh, S. M. Huang, B. T. Schurter, D. W. Aswad, and M. R. Stallcup.** 1999. Regulation of transcription by a protein methyltransferase. Science **284:**2174–2177.
17. **Chen, H., R. J. Lin, R. L. Schiltz, D. Chakravarti, A. Nash, L. Nagy, M. L. Privalsky, Y. Nakatani, and R. M. Evans.** 1997. Nuclear receptor coactivator ACTR is a novel histone acetyltransferase and forms a multimeric activation complex with P/CAF and CBP/p300. Cell **90:**569–580.
18. **Décimo, D., E. Georges-Labouesse, and P. Dollé.** 1995. In situ hybridisation to cellular RNA, p. 183–210. *In* B. D. Hames and J. S. Higgins (ed.), Gene probes, a practical approach, vol. II. Oxford University Press, New York, N.Y.
19. **de Rooij, D. G.** 2001. Proliferation and differentiation of spermatogonial stem cells. Reproduction **121:**347–354.
20. **Dierich, A. and. P. Dollé.** 1997. Gene targeting in embryonic stem cells, p. 111–123. *In* R. Klug and S. Thiel (ed.), Developmental toxicology and biology. Blackwell Science, Oxford, United Kingdom.
21. **Dupé, V., M. Davenne, J. Brocard, P. Dollé, M. Mark, A. Dierich, P. Chambon, and F. M. Rijli.** 1997. In vivo functional analysis of the Hoxa-1 3′ retinoic acid response element (3′RARE). Development **124:**399–410.
22. **Glass, C. K., and M. G. Rosenfeld.** 2000. The coregulator exchange in transcriptional functions of nuclear receptors. Genes Dev. **14:**121–141.
23. **Griswold, M. D.** 1995. Interactions between germ cells and Sertoli cells in the testis. Biol. Reprod. **52:**211–216.
24. **Griswold, M. D.** 1998. The central role of Sertoli cells in spermatogenesis. Semin. Cell Dev. Biol. **9:**411–416.
25. **Guillemot, F., A. Nagy, A. Auerbach, J. Rossant, and A. L. Joyner.** 1994. Essential role of Mash-2 in extraembryonic development. Nature **371:**333–336.
26. **Hogan, B., R. Beddington, F. Costantini, and E. Lacy.** 1994. Manipulating the mouse embryo, a laboratory manual. Cold Spring Harbor Laboratory Press, Cold Spring Harbor, N.Y.
27. **Hong, H., K. Kohli, A. Trivedi, D. L. Johnson, and M. R. Stallcup.** 1996. GRIP1, a novel mouse protein that serves as a transcriptional coactivator in yeast for the hormone binding domains of steroid receptors. Proc. Natl. Acad. Sci. USA **93:**4948–4952.
28. **Huang, H. F., and G. R. Marshall.** 1983. Failure of spermatid release under various vitamin A states: an indication of delayed spermiation. Biol. Reprod. **28:**1163–1172.
29. **Huang, S. M., and M. R. Stallcup.** 2000. Mouse Zac1, a transcriptional coactivator and repressor for nuclear receptors. Mol. Cell. Biol. **20:**1855–1867.
30. **Jacquemin, P., V. Sapin, E. Alsat, D. Evain-Brion, P. Dollé, and I. Davidson.** 1998. Differential expression of the TEF family of transcription factors in the murine placenta and during differentiation of primary human trophoblasts in vitro. Dev. Dyn. **212:**423–436.
31. **Jegou, B.** 1993. The Sertoli-germ cell communication network in mammals. Int. Rev. Cytol. **147:**25–96.
32. **Jimenez-Lara, A. M., M. J. Heine, and H. Gronemeyer.** 2000. Cloning of a mouse glucocorticoid modulatory element binding protein, a new member of the KDWK family. FEBS Lett. **468:**203–210.
33. **Kadonaga, J. T.** 1998. Eukaryotic transcription: an interlaced network of transcription factors and chromatin-modifying machines. Cell **92:**307–313.
34. **Kastner, P., M. Mark, M. Leid, A. Gansmuller, W. Chin, J. M. Grondona, D. Décimo, W. Krezel, A. Dierich, and P. Chambon.** 1996. Abnormal spermatogenesis in RXR beta mutant mice. Genes Dev. **10:**80–92.
35. **Kojima, S., M. Hatano, S. Okada, T. Fukuda, Y. Toyama,. Yuasa, H. Ito, and T. Tokuhisa.** 2001. Testicular germ cell apoptosis in Bcl6-deficient mice. Development **128:**57–65.
36. **Kozak, K. R., B. Abbott, and O. Hankinson.** 1997. ARNT-deficient mice and placental differentiation. Dev. Biol. **191:**297–305.
37. **Leo, C., and J. D. Chen.** 2000. The SRC family of nuclear receptor coactivators. Gene **245:**1–11.
38. **Li, H., P. J. Gomes, and J. D. Chen.** 1997. RAC3, a steroid/nuclear receptor-associated coactivator that is related to SRC-1 and TIF2. Proc. Natl. Acad. Sci. USA **94:**8479–8484.
39. **Lubahn, D. B., J. S. Moyer, T. S. Golding, J. F. Couse, K. S. Korach, and O. Smithies.** 1993. Alteration of reproductive function but not prenatal sexual development after insertional disruption of the mouse estrogen receptor gene. Proc. Natl. Acad. Sci. USA **90:**11162–11166.
40. **Lufkin, T., A. Dierich, M. LeMeur, M. Mark, and P. Chambon.** 1991. Disruption of the Hox-1.6 homeobox gene results in defects in a region corresponding to its rostral domain of expression. Cell **66:**1105–1119.
41. **Lufkin, T., D. Lohnes, M. Mark, A. Dierich, P. Gorry, M. P. Gaub, M. LeMeur, and P. Chambon.** 1993. High postnatal lethality and testis degeneration in retinoic acid receptor alpha mutant mice. Proc. Natl. Acad. Sci. USA **90:**7225–7229.
42. **Luo, J., R. Sladek, A. J. Bader, A. Matthyssen, J. Rossant, and V. Giguere.** 1997. Placental abnormalities in mouse embryos lacking the orphan nuclear receptor ERR-beta. Nature **388:**778–782.
43. **Maran, R. R., B. Ravisankar, K. Ravichandran, G. Valli, J. Arunakaran, and M. M. Aruldhas.** 1999. Impact of neonatal onset hypothyroidism on Sertoli cell number, plasma and testicular interstitial fluid androgen binding protein concentration. Endocr. Res. **25:**307–322.
44. **McKenna, N. J., R. B. Lanz, and B. W. O'Malley.** 1999. Nuclear receptor coregulators: cellular and molecular biology. Endocr. Rev. **20:**321–344.
45. **Metzger, D., and P. Chambon.** 2001. Site- and time-specific gene targeting in the mouse. Methods **24:**71–80.
46. **Metzger, D., J. Clifford, H. Chiba, and P. Chambon.** 1995. Conditional site-specific recombination in mammalian cells using a ligand-dependent chimeric Cre recombinase. Proc. Natl. Acad. Sci. USA **92:**6991–6995.
47. **Nait-Oumesmar, B., A. B. Copperman, and R. A. Lazzarini.** 2000. Placental expression and chromosomal localization of the human Gcm 1 gene. J. Histochem. Cytochem. **48:**915–922.
48. **Nistal, M., and R. Paniagua.** 1984. Testicular and epididymal pathology. Georg Thieme Verlag, New York, N.Y.
49. **Onate, S. A., S. Y. Tsai, M. J. Tsai, and B. W. O'Malley.** 1995. Sequence and characterization of a coactivator for the steroid hormone receptor superfamily. Science **270:**1354–1357.
50. **Palmero, S., P. De Marco, and E. Fugassa.** 1995. Thyroid hormone receptor beta mRNA expression in Sertoli cells isolated from prepubertal testis. J. Mol. Endocrinol. **14:**131–134.
51. **Puustinen, R., N. Sarvilinna, T. Manninen, P. Tuohimaa, and T. Ylikomi.** 2001. Localization of glucocorticoid receptor interacting protein 1 in murine tissues using two novel polyclonal antibodies. Eur. J. Endocrinol. **145:**323–333.
52. **Riley, P., L. Anson-Cartwright, and J. C. Cross.** 1998. The Hand1 bHLH transcription factor is essential for placentation and cardiac morphogenesis. Nat. Genet. **18:**271–275.
53. **Robyr, D., A. P. Wolffe, and W. Wahli.** 2000. Nuclear hormone receptor coregulators in action: diversity for shared tasks. Mol. Endocrinol. **14:**329–347.
54. **Rogatsky, I., K. A. Zarember, and K. R. Yamaoto.** 2001. Factor recruitment and TIF2/GRIP1 corepressor activity at a collagenase-3 response element that mediates regulation by phorbol esters and hormones. EMBO J. **20:**6071–6083.
55. **Rossant, J., and J. C. Cross.** 2001. Placental development: lessons from mouse mutants. Nat. Rev. Genet. **2:**538–548.
56. **Russell, L. D., A. P. S. Ettlin, and R. A. Clegg (ed.).** 1990. Histological and histopathological evaluation of the testis. Cache River Press, Clearwater, Fla.
57. **Sapin, V., P. Dollé, C. Hindelang, P. Kastner, and P. Chambon.** 1997. Defects of the chorioallantoic placenta in mouse RXRα null fetuses. Dev. Biol. **191:**29–41.
58. **Schulze, C., and A. F. Holstein.** 1993. Human Sertoli cell structure, p. 685–702. *In* L. D. Russell and M. D. Griswold (ed.), The Sertoli cell. Cache River Press, Clearwater, Fla.
59. **Sharpe, R. M.** 1993. Declining sperm counts in men—is there an endocrine cause? J. Endocrinol. **136:**357–360.
60. **Syed,V., and N. B. Hecht.** 1997. Up-regulation and down-regulation of genes

expressed in cocultures of rat Sertoli cells and germ cells. Mol. Reprod. Dev. **47:**380–389.
61. **Takeshita, A., G. R. Cardona, N. Koibuchi, C. S. Suen, and W. W. Chin.** 1997. TRAM-1, a novel 160-kDa thyroid hormone receptor activator molecule, exhibits distinct properties from steroid receptor coactivator-1. J. Biol. Chem. **272:**27629–27634.
62. **Torchia, J., D. W. Rose, J. Inostroza, Y. Kamei, S. Westin, C. K. Glass, and M. G. Rosenfeld.** 1997. The transcriptional co-activator p/CIP binds CBP and mediates nuclear-receptor function. Nature **387:**677–684.
63. **Veeck, L.** 1998. An atlas of human gametes and conceptuses. Parthenon Publishing Group, New York, N.Y.
64. **Voegel, J. J., M. J. Heine, C. Zechel, P. Chambon, and H. Gronemeyer.** 1996. TIF2, a 160 kDa transcriptional mediator for the ligand-dependent activation function AF-2 of nuclear receptors. EMBO J. **15:**3667–3675.
65. **Voegel, J. J., M. J. Heine, M. Tini, V. Vivat, P. Chambon, and H. Gronemeyer.** 1998. The coactivator TIF2 contains three nuclear receptor-binding motifs and mediates transactivation through CBP binding-dependent and -independent pathways. EMBO J. **17:**507–519.
66. **Wang, Z., D. W. Rose, O. Hermanson, F. Liu, T. Herman, W. Wu, D. Szeto, A. Gleiberman, A. Krones, K. Pratt, R. Rosenfeld, C. K. Glass, and M. G. Rosenfeld.** 2000. Regulation of somatic growth by the p160 coactivator p/CIP. Proc. Natl. Acad. Sci. USA **97:**13549–13554.
67. **Weiss, R. E., J. Xu, G. Ning, J. Pohlenz, B.W. O'Malley, and S. Refetoff.** 1999. Mice deficient in the steroid receptor co-activator 1 (SRC-1) are resistant to thyroid hormone. EMBO J. **18:**1900–1904.
68. **Wendling, O., P. Chambon, and M. Mark.** 1999. Retinoid X receptors are essential for early mouse development and placentogenesis. Proc. Natl. Acad. Sci. USA **96:**547–551.
69. **Westin, S., M. G. Rosenfeld, and C. K. Glass,C.K.** 2000. Nuclear receptor coactivators. Adv. Pharmacol. **47:**89–112.
70. **Wolffe, A. P. E.** 2001. Chromatin remodeling. Oncogene **20:**2987–3172.
71. **Wright, W. W., S. D. Zabludoff, T. L. Penttila, and M. Parvinen.** 1995. Germ cell-Sertoli cell interactions: regulation by germ cells of the stage-specific expression of CP-2/cathepsin L mRNA by Sertoli cells. Dev. Genet. **16:**104–113.
72. **Xu, J., L. Liao, G. Ning, H. Yoshida-Komiya, C. Deng, and B. W. O'Malley.** 2000. The steroid receptor coactivator SRC-3 (p/CIP/RAC3/AIB1/ACTR/TRAM-1) is required for normal growth, puberty, female reproductive function, and mammary gland development. Proc. Natl. Acad. Sci. USA **97:**6379–6384.
73. **Xu, J., Y. Qiu, F. J. DeMayo, S. Y. Tsai, M. J. Tsai, and B. W. O'Malley.** 1998. Partial hormone resistance in mice with disruption of the steroid receptor coactivator-1 (SRC-1) gene. Science **279:**1922–1925.
74. **Xu, L., C. K. Glass, and M. G. Rosenfeld.** 1999. Coactivator and corepressor complexes in nuclear receptor function. Curr. Opin. Genet. Dev. **9:**140–147.
75. **Yomogida, K., H. Ohtani, H. Harigae, E. Ito, Y. Nishimune, J. D. Engel, and M. Yamamoto.** 1994. Developmental stage- and spermatogenic cycle-specific expression of transcription factor GATA-1 in mouse Sertoli cells. Development **120:**1759–1766.